Electronic Supplementary Material (ESI) for Journal of Materials Chemistry A.

New Insight into Li/Ni Disorder in Layered Cathode Materials for Lithium ion Battery: A Joint Study of Neutron Diffraction, Electrochemical Kinetics Analysis and First-principles Calculations

Enyue Zhao[1], Lincan Fang[1], Minmin Chen[1], Dongfeng Chen[2], Qingzhen Huang[3], Zhongbo Hu[1], Qing-bo Yan [*1], Meimei Wu [*2], Xiaoling Xiao [*1]

[1]College of Materials Science and Opto-electronic Technology University of Chinese Academy of Sciences, Beijing 100049, P. R. China. E-mail: xlxiao@ucas.ac.cn. Tel. +86 10 8825 6653, E-mail: yan@ucas.ac.cn. Tel. +86 10 8825 6655;

[2]Department of Nuclear Physics, China Institute of Atomic Energy, 102413, Beijing, P. R. China. E-mail: mmwuciae@126.com, Tel: +86 10 6935 8015;

[3]NIST Center for Neutron Research, NIST, Gaithersburg, 20899-6102, Maryland, USA

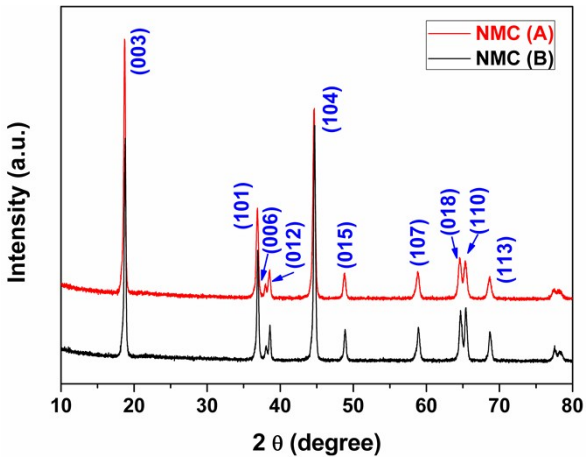

Figure SI 1. XRD patterns of $LiNi_{1/3}Mn_{1/3}Co_{1/3}O_2$.

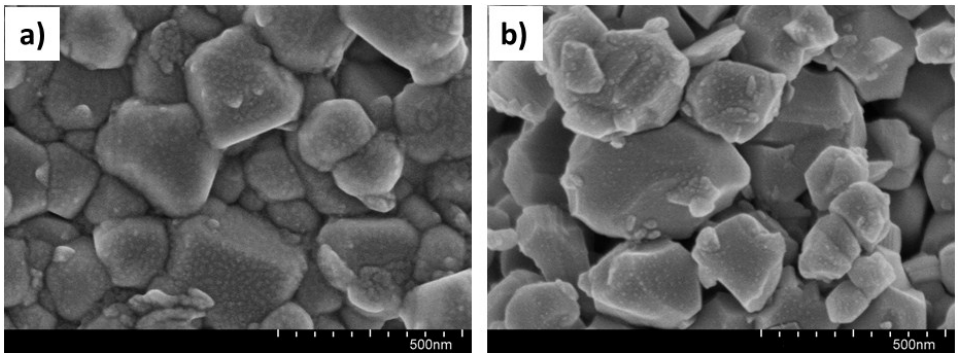

Figure SI 2. SEM images of a) NMC (A) and b) NMC (B).

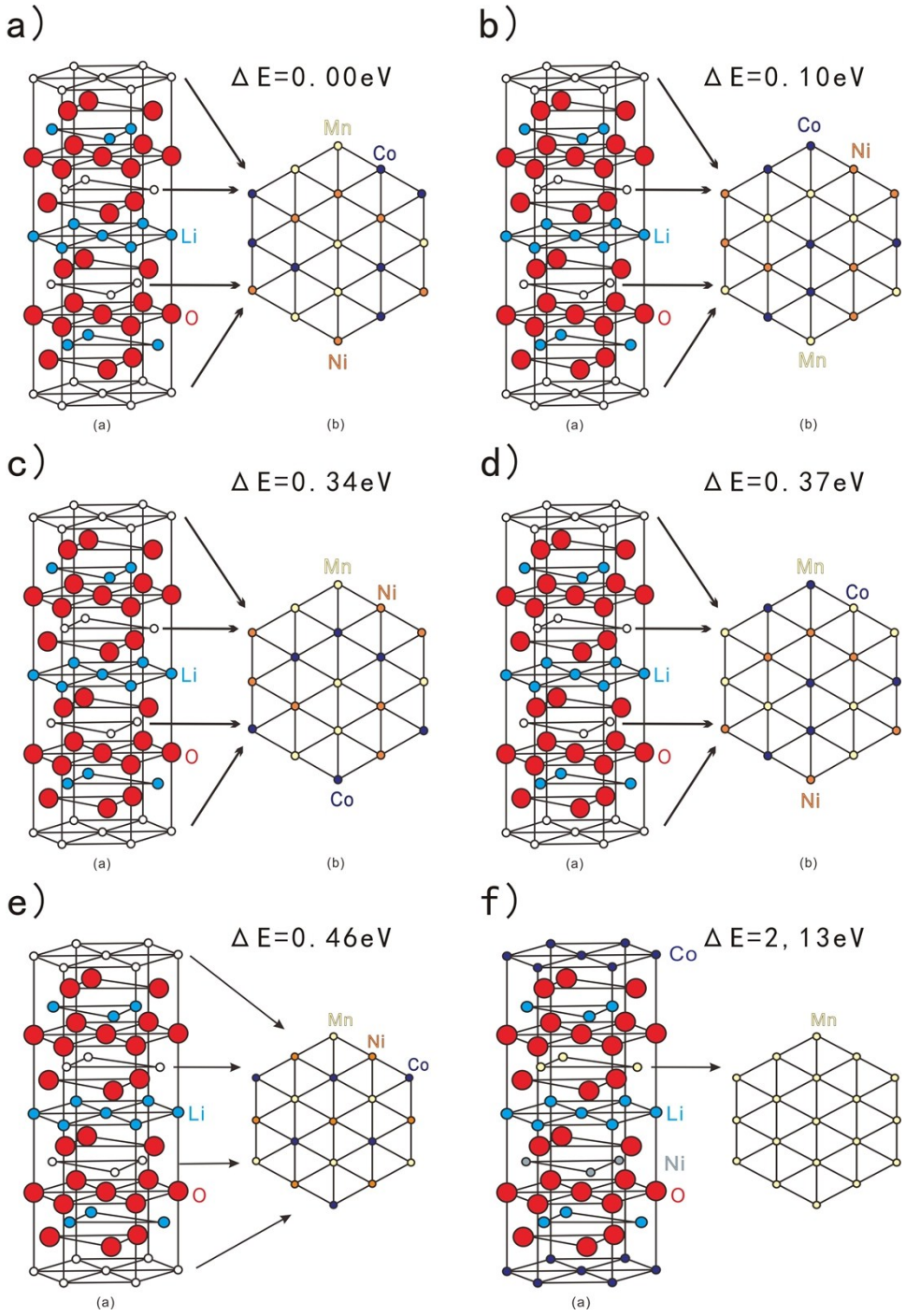
a)
ΔE=0.00eV
Mn
Co
Li
O
Ni
(a)
(b)
b)
ΔE=0.10eV
Co
Ni
Li
O
Mn
(a)
(b)
c)
ΔE=0.34eV
Mn
Ni
Li
O
Co
(a)
(b)
d)
ΔE=0.37eV
Mn
Co
Li
O
Ni
(a)
(b)
e)
ΔE=0.46eV
Mn
Ni
Co
Li
O
(a)
f)
Co
ΔE=2,13eV
Mn
Li
Ni
O
(a)

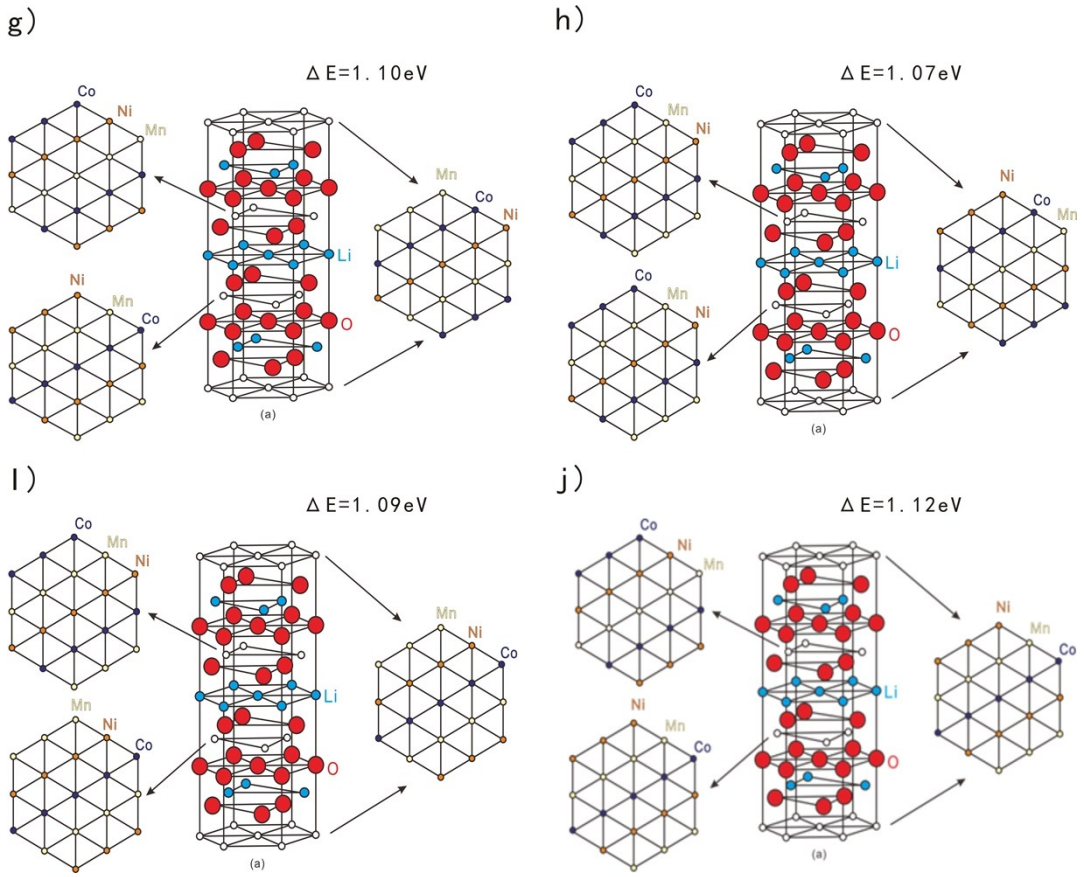

Figure SI 3. The schematic structures and calculated relative energies of $LiNi_{1/3}Mn_{1/3}Co_{1/3}O_2$ crystal with different Co, Ni, Mn ordering patterns.

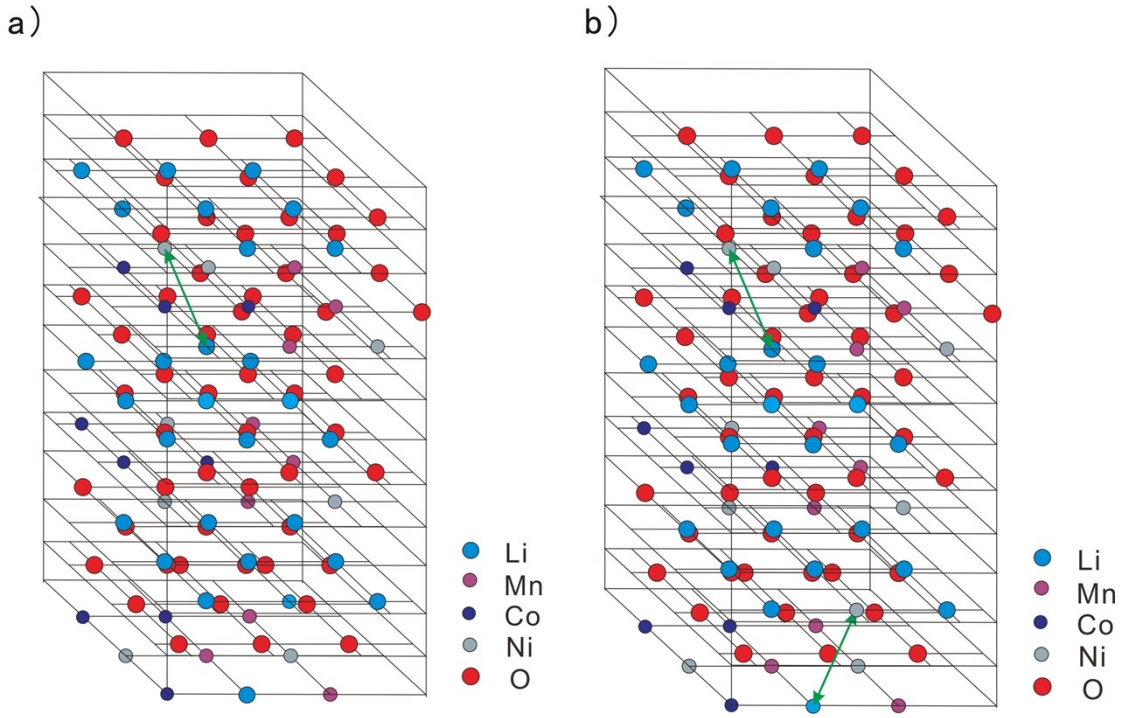

Figure SI 4. The schematic structure of $LiNi_{1/3}Mn_{1/3}Co_{1/3}O_2$ crystal with (a) 3.7% and (b) 7.4% Li^+/Ni^{2+} ion exchange. The arrows indicated the exchanged atoms in the models.

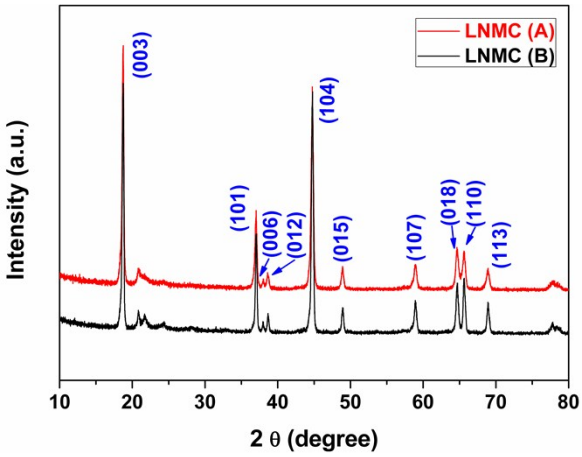

Figure SI 5. XRD patterns of $Li_{1.2}Mn_{0.54}Ni_{0.13}Co_{0.13}O_2$.

All the peaks can be well indexed to a hexagonal $NaFeO_2$ structure with space group R-3m and monoclinic system with space group C2/m. Weak superstructure reflection peaks appeared between 20° and 25° are characteristic of lithium-enriched nickel manganese oxides.

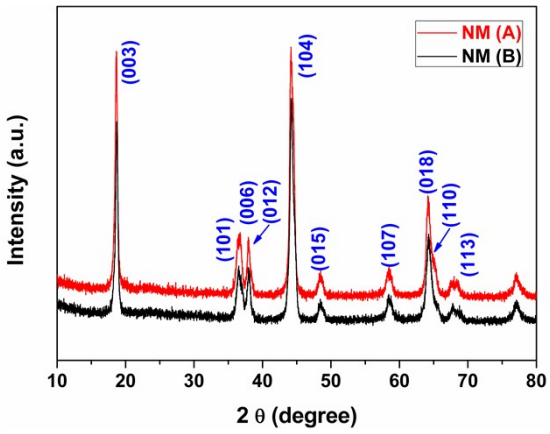

Figure SI 6. XRD patterns of $LiNi_{0.5}Mn_{0.5}O_2$.

All the peaks can be well indexed to a hexagonal $NaFeO_2$ structure with space group R-3m.

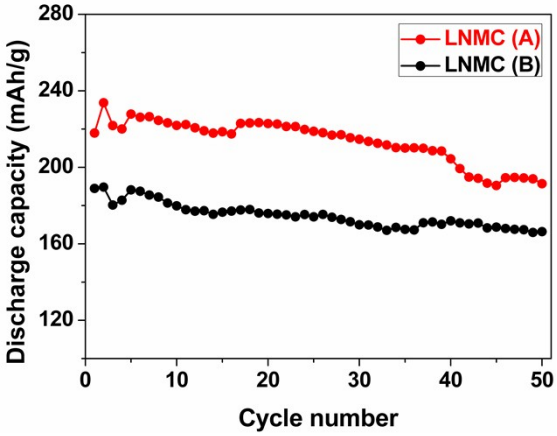

Figure SI 7. Cycle performance of LNMC (A) and LNMC (B) at the current density of 40 mA/g

after activation at 20 mA/g for 2 cycles.

It can be seen in Figure SI 7 that the discharge capacity of LNMC (A) and LNMC (B) is 191 and 166 mA h/g, respectively, after 50 cycles.

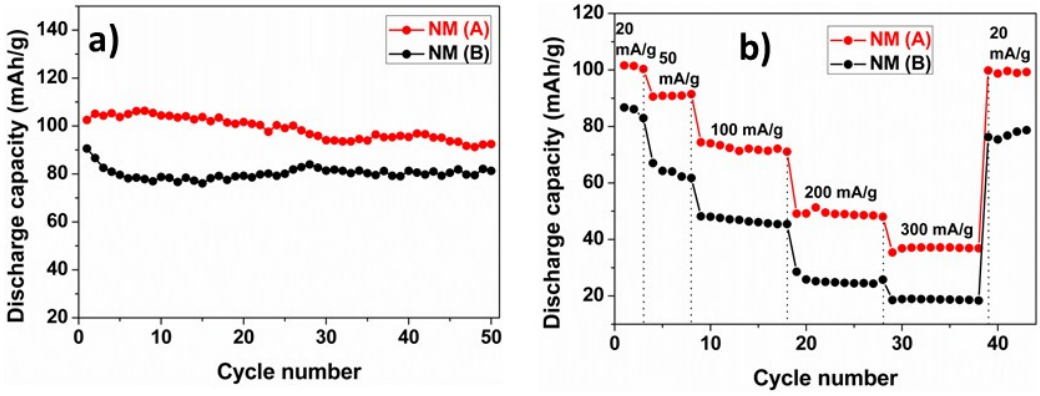

Figure SI 8. a) Cycle performance of NM (A) and NM (B) at the current density of 40 mA/g, b) rate performance of NM (A) and NM (B) at different current densities.

It can be seen in Figure SI 8 that the discharge capacity of NM (A) and NM (B) is 93 and 81 mA h/g, respectively, after 50 cycles. Meanwhile, in comparison with NM (B), NM (A) also show better rate capability. At the current density of 300 mA/g. the discharge capacity of NM (A) is 37 mA h/g, while that of NM (B) is only 18 mA h/g.

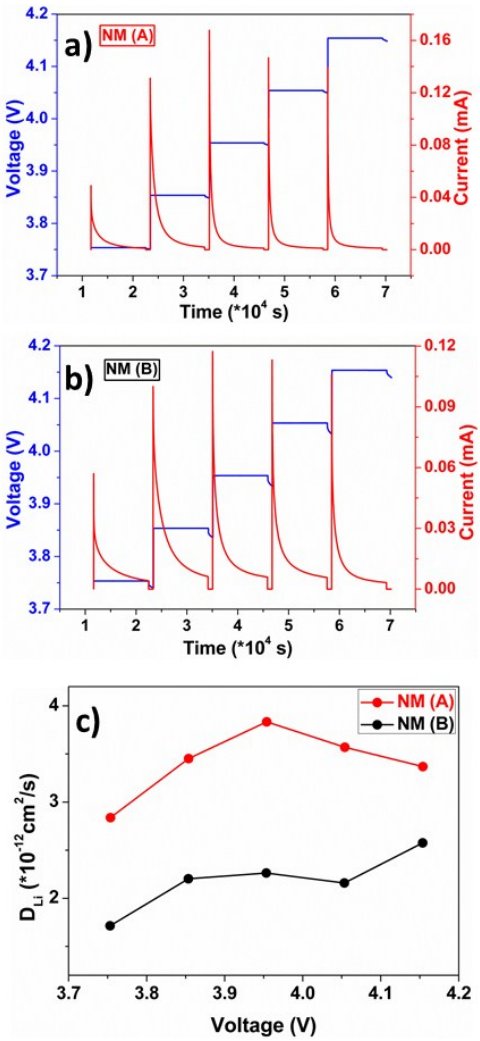

Figure SI 9. The relationship of the transition current (I) depending on the titration time (t) at different charge potentials. (a) NM (A), (b) NM (B), and (c) the comparison of the lithium diffusion coefficient.

It can be seen in Figure SI 9 that the average D_{Li} of NM (A) is 3.5E-12 cm^2/s, while that of NM (B) is 2.2E-12 cm^2/s.

Table SI 1 ICP results (molar percentage content) of NMC (A) and NMC (B)

Samples	Li	Ni	Mn	Co
NMC (A)	1.01%	0.33 %	0.32 %	0.33 %
NMC (B)	1.02%	0.33 %	0.33 %	0.33 %

Table SI 2 The fitted solution resistances (R_s) and charge transfer resistances (R_{ct}) for the Nyquist plots of NMC and LNMC before cycling.

Samples	R_s (Ω)	R_{ct} (Ω)
NMC (A)	0.963	81.448
NMC (B)	2.018	129.020
LNMC (A)	2.122	201.750
LNMC (B)	2.422	269.690